



Original scientific paper

## Electrochemical micromachining of galvanized iron sheets: process optimization and performance evaluation

Nadanasabapathi Sivashankar<sup>1,✉</sup>, Kadhiresan Santhanam<sup>2</sup>, Shikandar Prasad<sup>3</sup>, Mamidala Jawahar<sup>4</sup> and Rajasekaran Thanigaivelan<sup>5</sup>

<sup>1</sup>Department of Mechanical Engineering, Kongunadu College of Engineering and Technology (Autonomous), Trichy, Tamilnadu 621215 India

<sup>2</sup>K. S. Rangasamy College of Technology, Tiruchengode, Namakkal, Tamil Nadu 637215, India

<sup>3</sup>Government Engineering College, Nawada, Bihar 805110, India

<sup>4</sup>Department of Mechanical Engineering, Jayamukhi Institute of Technological Sciences, Narsampet, Warangal, Telangana 506332, India

<sup>5</sup>Department of Mechanical Engineering, Shreenivasa Engineering College, Bommidi, Dharmapuri, Tamilnadu 635301, India

Corresponding Author: ✉ [sivashankar1911@gmail.com](mailto:sivashankar1911@gmail.com)

Received: May 30, 2025; Revised: July 28, 2025; Published: July 31, 2025

### Abstract

Electrochemical micromachining (ECMM) is a promising non-traditional technique for fabricating micro-features on conductive materials with high precision and minimal thermal effects. This study focuses on the ECMM of galvanized iron (GI) sheets using sodium nitrate ( $\text{NaNO}_3$ ) as the electrolyte. Key process parameters such as voltage, duty cycle, and electrolyte concentration were optimized to improve machining performance in terms of material removal rate (MRR) and overcut (OC). An L9 orthogonal array was used to design the experiments, and signal-to-noise ratio, along with analysis of variance (ANOVA), was employed to identify the most influential parameters. Results showed that voltage significantly influenced both MRR and OC, with optimal MRR observed at 12 V, 70 % duty cycle, and 20 g l<sup>-1</sup>  $\text{NaNO}_3$  concentration. Conversely, the minimum OC was achieved at 6 V, 50 % duty cycle and 10 g l<sup>-1</sup>  $\text{NaNO}_3$  electrolyte concentration. SEM analysis confirmed over-etched boundaries at higher voltage and well-defined micro-holes at lower voltage. This research demonstrates the critical role of parameter tuning in enhancing the quality and precision of ECMM on GI sheets.

### Keywords

Galvanized steel; electrochemical material removal; machining parameters; removal rate; overcut

## Introduction

Electrochemical micromachining (ECMM) is a non-traditional machining process that utilizes electrochemical reactions to remove material from a workpiece. It is particularly effective for machining hard-to-cut materials with complex geometries. In ECMM, a tool electrode and the workpiece are separated by an electrolyte, and an electric current is passed through the electrolyte to dissolve material from the workpiece [1,2]. This process is advantageous as it generates minimal heat, reducing thermal stresses and avoiding tool wear. However, achieving precise control over the machining parameters is crucial to obtain desired outcomes [3,4]. Galvanized iron (GI) sheets are widely used in various applications due to their high corrosion resistance and mechanical properties. The zinc coating on GI sheets provides enhanced durability but also introduces challenges in machining. The electrochemical behaviour of the zinc layer can differ from that of the underlying iron, leading to variations in material removal rates and surface finishes. Understanding the interaction between the electrolyte, zinc coating, and underlying iron is essential for optimizing ECMM parameters for GI sheets [5-7]. Several researchers have conducted experimental studies in ECMM by introducing various innovations to enhance machining performance. Maniraj & Thanigaivelan [8] investigated the effect of heated electrolyte on the machining of aluminium workpiece using the ECMM process. The use of heated electrolytes improves the MRR by 88.37 % and reduces radial OC by 37.03 %.  $\text{NaNO}_3$  was reported to offer high performance as an electrolyte for aluminium machining. Vinod Kumar and Thanigaivelan [9] applied magnetic fields in the electrolyte during ECMM of SS316L stainless steel. Their study revealed that a magnetic field-assisted citric acid electrolyte resulted in a 4.87 % reduction in OC compared to conventional NaCl electrolytes. They also identified the optimal machining parameters as 7 V, 85 % duty cycle, and  $20 \text{ g l}^{-1}$  electrolyte concentration for machining SS316L. Soundarrajan & Thanigaivelan [10] studied the machining parameters and the effects of using a coated tool in the ECMM process. Their experimental results demonstrated that a ceramic-coated tool produced a minimum OC, reducing it by 43.1 % under the machining conditions of 15 V, 23 g/l electrolyte concentration, and 85 % duty cycle. Venugopal & Thanigaivelan [11] investigated the performance of a magnetized tool in ECMM on scrapped alloy material. Their findings revealed that the magnetized tool had a significant positive impact on the MRR. Ge *et al.* [12] improved ECMM performance through energy conversion. They found that modifying the degree of convergence of the electrolyte outlet significantly impacts the MRR and OC. Deepak and Hariharan [13] investigated ECMM performance on SS304 stainless steel using NaCl and  $\text{NaNO}_3$  electrolytes. They stated that the applied voltage has a major impact during machining with a hollow tool. Most experiments were conducted using submerged-type machining, where the workpiece is immersed in the electrolyte. However, due to the galvanic corrosion nature of magnesium alloy, this traditional approach is not suitable for ECMM of magnesium alloys [14]. Sivashankar & Thanigaivelan [15] proposed a novel machining method for magnesium alloy by supplying a minimum quantity of electrolyte to the machining zone. They found that the citric acid electrolyte performed better compared to the  $\text{NaNO}_3$  electrolyte.

Optimization of machining parameters is essential to determine the most suitable machining conditions. Various optimization techniques are available, such as single-objective and multi-objective optimization, Grey relational coefficient (GRC), generalized reduced gradient (GRG), and Technique for order of preference by similarity to ideal solution (TOPSIS) [16]. Among these, single-objective and multi-objective optimization methods are particularly effective in materials research [17]. Optimization of ECMM parameters for GI sheets is a complex task that involves understanding the interplay between various process parameters and the materials' properties. While significant

advancements have been made in ECMM, there is a need for focused research on GI sheets to develop tailored optimization strategies. Such research will contribute to more efficient and precise machining of GI sheets, expanding the applicability of ECMM in various industries.

## Experimental

The workpiece material used for the ECMM process was a GI sheet with a thickness of 2 mm. The GI sheet samples were cut into rectangular specimens of dimensions 15×20 mm using precision shearing to ensure uniformity and minimize edge defects. Galvanized iron was selected due to its wide industrial usage, corrosion resistance, and machinability challenges in conventional methods. A solid cylindrical steel tool with a diameter of 600  $\mu\text{m}$  was employed as the cathodic electrode. The tool was chosen for its good electrical conductivity, corrosion resistance, and dimensional stability during the machining process. The electrode was mounted vertically and aligned precisely to ensure concentric machining. The circumference of the tool electrode was coated with an insulating epoxy resin to mitigate the effects of stray currents. This coating serves to confine the electrochemical reaction primarily to the tool's front face by preventing current leakage along the tool's sidewalls.  $\text{NaNO}_3$  solution was used as the electrolyte. The solution was prepared by dissolving a predetermined concentration of  $\text{NaNO}_3$  in distilled water, ensuring homogeneity through constant stirring.  $\text{NaNO}_3$  was selected due to its effective oxidation behaviour, moderate conductivity, and environmental safety compared to other electrolytes. The machining operations were conducted on a custom-built in-house setup developed by Sivasakthy Electricals, Salem, Tamil Nadu, India, specifically designed to perform precision micromachining. The setup included a tool feed mechanism, an electrolyte delivery system, and a work holding fixture. The GI workpiece was connected as the anode and the steel tool electrode as the cathode. Electrolyte was circulated continuously through the inter-electrode gap to remove reaction by-products and to maintain uniform machining conditions. The developed setup is illustrated in Figure 1

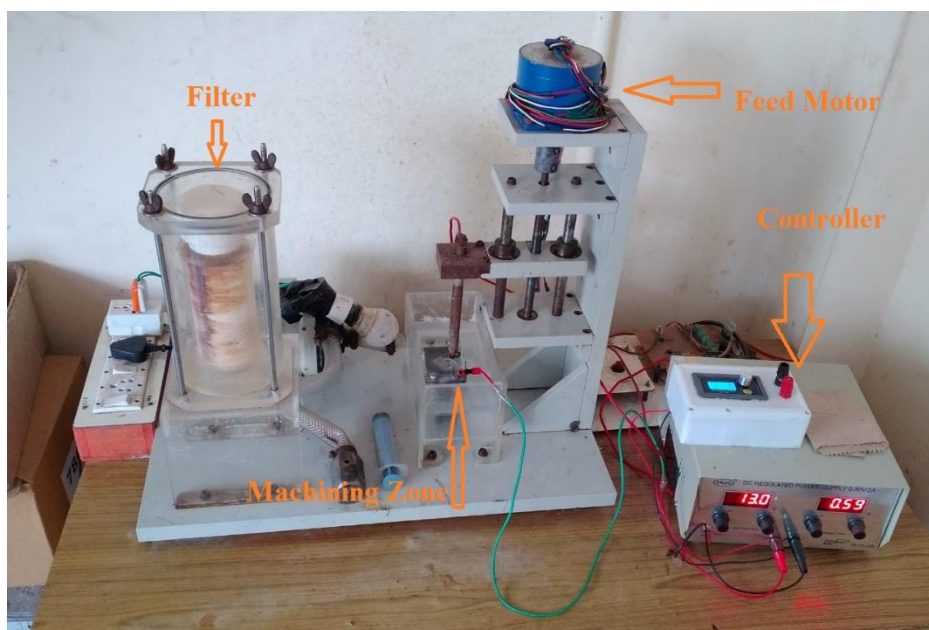


**Figure 1.** Machine setup

The machining was performed by systematically varying the process parameters such as voltage, electrolyte concentration (EC) and duty cycle. The selected parameters and their levels are presented in Table 1.

**Table 1.** ECMM process parameters.

Parameter	Level		
	1	2	3
ECMM voltage, V	6	9	12
Duty cycle, %	50	60	70
Concentration of NaNO <sub>3</sub> electrolyte, g l <sup>-1</sup>	10	20	30

## Results and discussion

### Definitions of optimization

To analyse the effects of input parameters on material removal rate (MRR) and overcut (OC), Taguchi's optimization approach, along with analysis of variance (ANOVA) was employed. The signal-to-noise (*S/N*) ratio, a key measure in Taguchi analysis, was used to identify the optimal settings of control factors by minimizing variability in the response. For MRR, the larger-the-better *S/N* criterion was applied, whereas for OC, the smaller-the-better criterion was adopted. The mean of means represents the average response value at each level of the input factors. In ANOVA, several statistical parameters were considered: degrees of freedom (DF) represent the number of independent comparisons, adjusted sum of squares (Adj SS) quantifies the variation explained by each factor, adjusted mean square (Adj MS) is obtained by dividing SS by its corresponding DF, the *F*-value indicates the significance of each factor's effect and the *p*-value denotes statistical significance with values below 0.05 indicating a strong influence. Additionally, *R*<sup>2</sup> (coefficient of determination) reflects the goodness of fit of the model while adjusted *R*<sup>2</sup> and predicted *R*<sup>2</sup> assess its explanatory and predictive capabilities, respectively.

For the experimental design, the L9 orthogonal array (OA) was employed, and its results are presented in Table 2.

**Table 2.** L9 design and outputs

S. No	Voltage, V	Duty cycle, %	EC, g l <sup>-1</sup>	MRR, μm s <sup>-1</sup>	OC, μm	<i>S/N</i>	
						MRR	OC
1	6	50	10	0.476	18	-6.44786	-25.1055
2	9	60	20	0.741	22	-2.60364	-26.8485
3	12	70	30	0.901	27	-0.90550	-28.6273
4	6	50	30	0.556	24	-5.09850	-27.6042
5	9	60	10	0.833	20	-1.58710	-26.0206
6	12	70	20	1.042	26	0.35735	-28.2995
7	6	50	20	0.641	21	-3.86284	-26.4444
8	9	60	30	0.855	25	-1.36068	-27.9588
9	12	70	10	1.190	24	1.51094	-27.6042

### Effect of machining parameters on material removal rate

Voltage exhibited the most significant impact on the MRR. As the applied voltage increased from 6 to 12 V, the MRR showed a consistent and marked increase at all electrolyte concentrations. For instance, at 10 g l<sup>-1</sup> NaNO<sub>3</sub> concentration, the MRR rose from 0.476 μm s<sup>-1</sup> at 6 V to 1.190 μm s<sup>-1</sup> at 12 V. This rise is attributed to the higher electric potential promoting faster anodic dissolution at the workpiece surface. In ECMM, the rate of electrochemical reactions and material removal is directly proportional to the current density, which increases with applied voltage [18]. The intensified electric field enhances the mobility of ions in the electrolyte, accelerating the dissolution of the GI surface and thus increasing MRR.

The duty cycle significantly influenced MRR. A higher duty cycle means a longer pulse-on time relative to the total pulse period, allowing for sustained ion transfer and prolonged anodic activity during each cycle. At 9 V and 10 g l<sup>-1</sup> concentration, for example, the MRR increased from 0.833 μm s<sup>-1</sup> at 60 % duty cycle to 1.042 μm s<sup>-1</sup> at 70 %. This improvement is a direct result of the extended reaction time, enabling more material to be dissolved in each machining pulse.

Electrolyte concentration, ranging from 10 to 30 g l<sup>-1</sup> of NaNO<sub>3</sub>, also played a notable role in influencing MRR. A general trend of increasing MRR with rising concentration was evident, though the effect was not as pronounced as the voltage effect. At 12 V and 70 % duty cycle, MRR increased to 1.042 μm s<sup>-1</sup> at 20 g l<sup>-1</sup> and then slightly decreased to 0.901 μm s<sup>-1</sup> at 30 g l<sup>-1</sup>. This non-linear behaviour suggests that increasing NaNO<sub>3</sub> concentration enhances electrolyte conductivity and ion availability, while excessively high concentrations may cause polarization or side reactions near the tool, diminishing the effective dissolution rate [19]. The optimal ion concentration is therefore crucial for maintaining a stable and efficient reaction zone.

A single-objective optimization was carried out to identify the most influential input parameters affecting the MRR. The *S/N* ratio for MRR was calculated using Minitab software 2019 (<https://www.minitab.com/en-us/products/minitab/>) and the results are presented in Table 2. Based on the computed *S/N* ratios, main effects plots were generated and are shown in Figures 2 and 3.

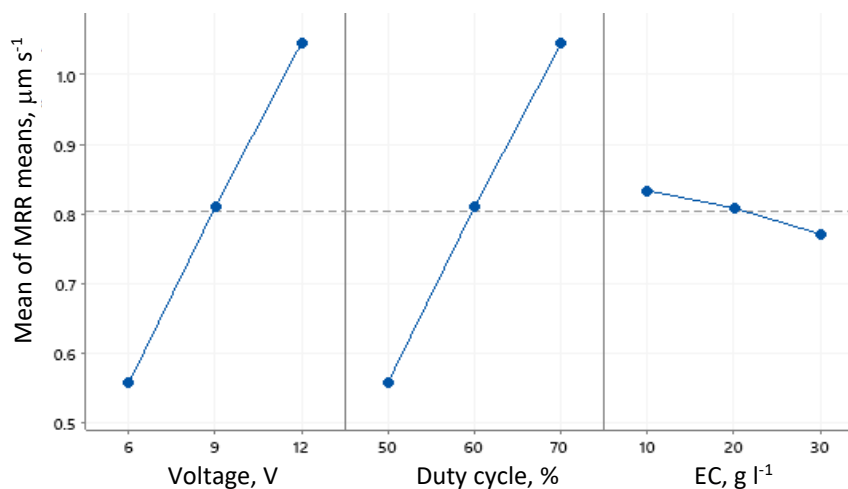


**Figure 2.** Main effects plot for MRR mean

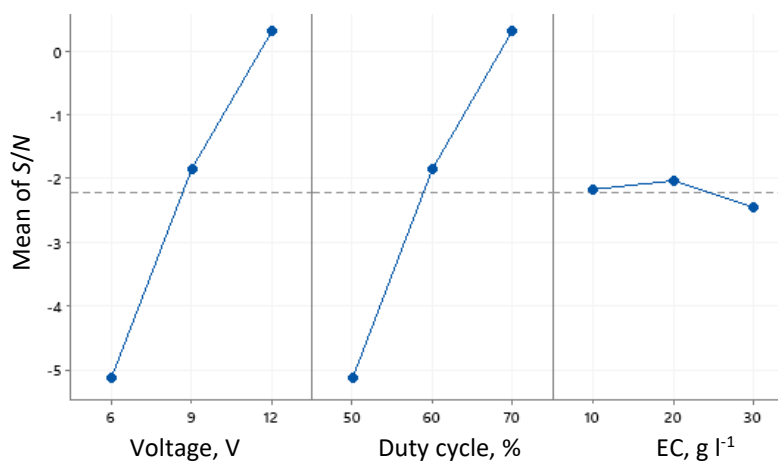


**Figure 3.** Main effect plot MRR-S/N ratio

To maximize the average MRR, the main effects plot for mean (Figure 2) is utilized, whereas the main effects plot for *S/N* ratio (Figure 3) is employed to select parameter levels that offer stable and consistent MRR under varying conditions. These plots indicate that voltage has a notable impact on

MRR. Specifically, MRR increases with rising voltage from 6 to 12 V, demonstrating a positive correlation between applied voltage and machining efficiency. This can be attributed to enhanced electrochemical reaction kinetics at higher voltages, which promote faster material dissolution.

Interaction plots are used to determine whether two factors exhibit interaction, which occurs when the effect of one factor varies depending on the level of another. If the lines are parallel, it indicates that there is no significant interaction between the factors, meaning the influence of one factor remains consistent across all levels of the other. The interaction plot for MRR (Figure 4) reveals minimal interaction between voltage and electrolyte concentration, as indicated by the absence of significant line intersections. This suggests that voltage influences MRR independently of other parameters, and variations in electrolyte concentration do not notably affect this relationship. To further validate these observations, an ANOVA was conducted, with the results summarized in Table 3. The ANOVA results confirm that voltage significantly affects MRR, with a *p*-value of 0.019. In contrast, the electrolyte concentration has a *p*-value of 0.821, indicating that it has an insignificant effect on MRR within the tested range. The computed *R*<sup>2</sup> of 86.42 % indicates that the model accounts for a substantial portion of the variability in MRR. Based on the results from ANOVA and single-objective optimization, the most optimal and influential set of process parameters for maximizing MRR was identified as a voltage of 12 V, a duty cycle of 70 % and NaNO<sub>3</sub> electrolyte concentration of 20 g l<sup>-1</sup>. Confirmation experiments were conducted using the optimal process parameters, and the SEM image of the machined microhole on the GI sheet is presented in Figure 5. As observed in the image, the sample exhibits an over-etched boundary layer, which can be attributed to the rapid movement of ions at the high machining voltage.

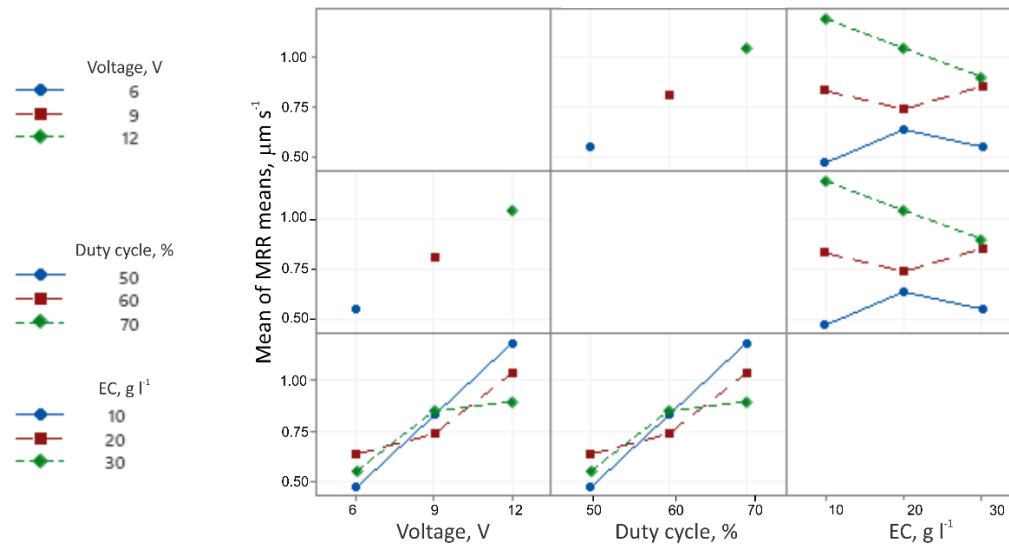
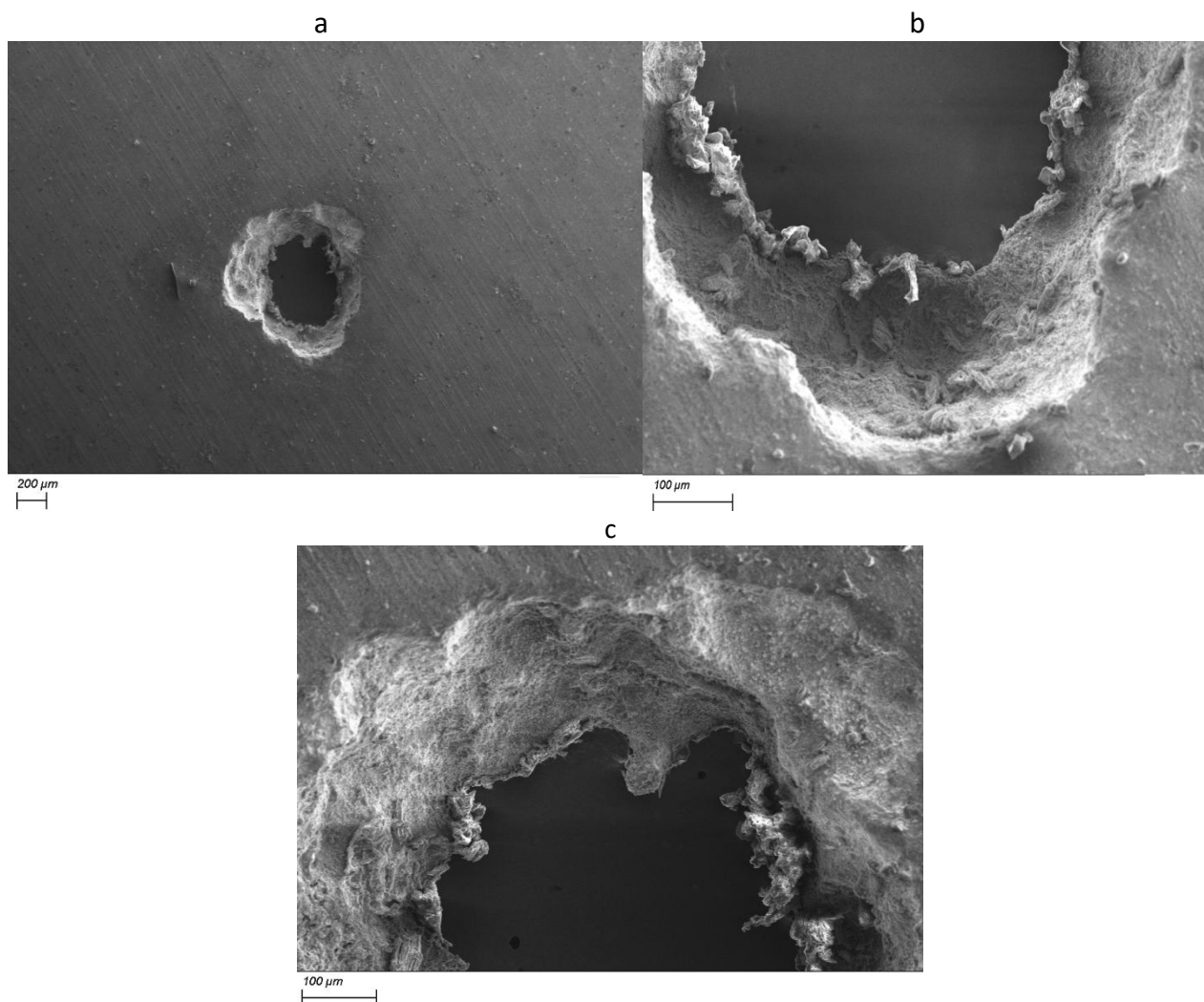


Figure 4. Interaction plot of MRR

Table 3. Analysis of variance-MRR

Source	Degree of freedom	Adj SS	Adj MS	F-value	<i>p</i> -value
Voltage	2	0.355417	0.177708	12.52	0.019
EC	2	0.005904	0.002952	0.21	0.821
Error	4	0.056796	0.014199		
Total	8	0.418117			



**Figure 5.** SEM images at optimal input parameter-MRR: a - machined microhole; b - microhole profile; c - microhole with over-etched boundary

#### *Effect of machining parameters on overcut*

The OC, a measure of dimensional inaccuracy caused by lateral material removal beyond the intended profile, was also strongly influenced by the process parameters. As with MRR, voltage exerted the greatest influence on OC. An increase in voltage from 6 to 12 V generally resulted in a higher OC. At 10 g l<sup>-1</sup> electrolyte concentration, the OC rose from 18 μm at 6 V to 24 μm at 12 V. This is explained by the radial spread of the electric field at higher voltages, which causes ion migration and anodic dissolution beyond the tool boundary [20]. In ECMM, unlike in mechanical micro-machining, the electric field is not strictly confined to the tool geometry, especially at higher voltages where field lines diverge more aggressively, contributing to lateral etching and increased OC. Duty cycle had a similar influence on OC. At a fixed voltage and concentration, increasing the duty cycle led to more extensive material removal around the tool periphery. At 9 V and 30 g l<sup>-1</sup> concentration, OC increased from 25 μm at 60 % duty cycle to 27 μm at 70 %. The prolonged pulse duration allows the electrochemical reaction to act not only axially but also radially, particularly when the electrolyte replenishment is not sufficiently fast to maintain a narrow reaction zone. Thus, although higher duty cycles improve MRR, they reduce geometric precision. Electrolyte concentration also impacted OC, though its effect was more moderate compared to voltage and duty cycle. Increasing NaNO<sub>3</sub> concentration from 10 to 30 g l<sup>-1</sup> resulted in a gradual rise in OC. At 6 V and 50 % duty cycle, for instance, OC increased from 18 μm at 10 g l<sup>-1</sup> to 24 μm at 30 g l<sup>-1</sup>. The enhanced

conductivity at higher concentrations facilitates greater current spread, including lateral flow paths that cause unwanted etching. Moreover, a highly concentrated electrolyte may lower the localization of the dissolution process, making it harder to maintain sharp boundaries [21].

To evaluate the dimensional accuracy of electrochemical micromachining on a GI sheet, OC was considered as a key response parameter. The influence of voltage and electrolyte concentration on OC was analysed using *S/N* ratio plots, interaction plots and ANOVA. The *S/N* ratios were calculated using Minitab software, and optimization was performed to minimize OC. The mean of means is the average of the mean overcut values calculated at each level of the input factors. Mean of *S/N* ratio is used to identify parameter settings that yield low and consistent overcut, which is critical for precision machining. Figures 6 and 7 present the main effects plots for OC (mean and *S/N* ratio, respectively). From these plots, it is evident that both voltage and electrolyte concentration significantly affect the OC. As voltage increases from 6 to 12 V, the OC also increases, which can be attributed to enhanced ion mobility and greater material dissolution around the edges of the machined feature. Similarly, electrolyte concentration exhibits a trend where OC increases with concentration, particularly at a concentration of 30 g l<sup>-1</sup>. This suggests that higher ion density in the electrolyte leads to greater lateral etching, contributing to increased OC.

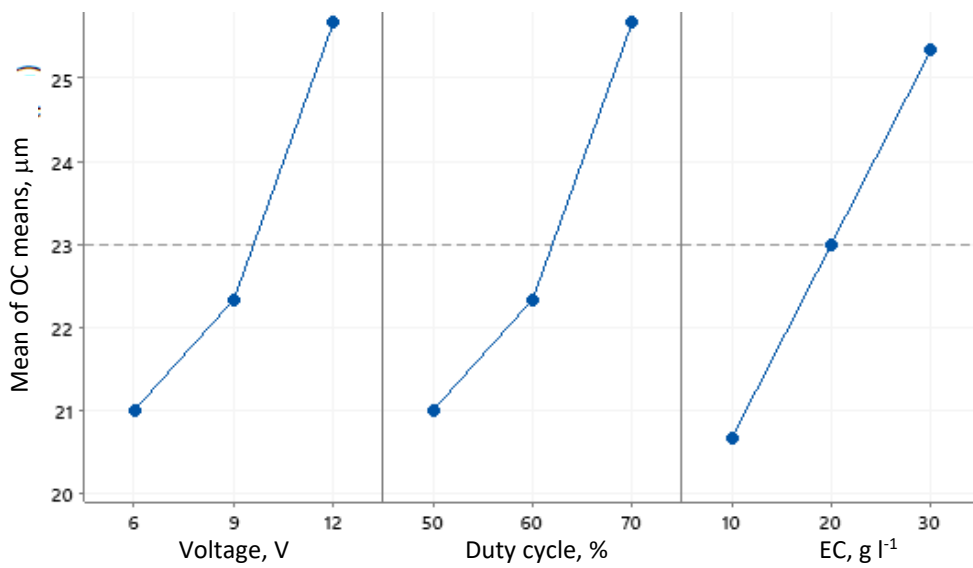


Figure 6. Main effects plots OC - mean

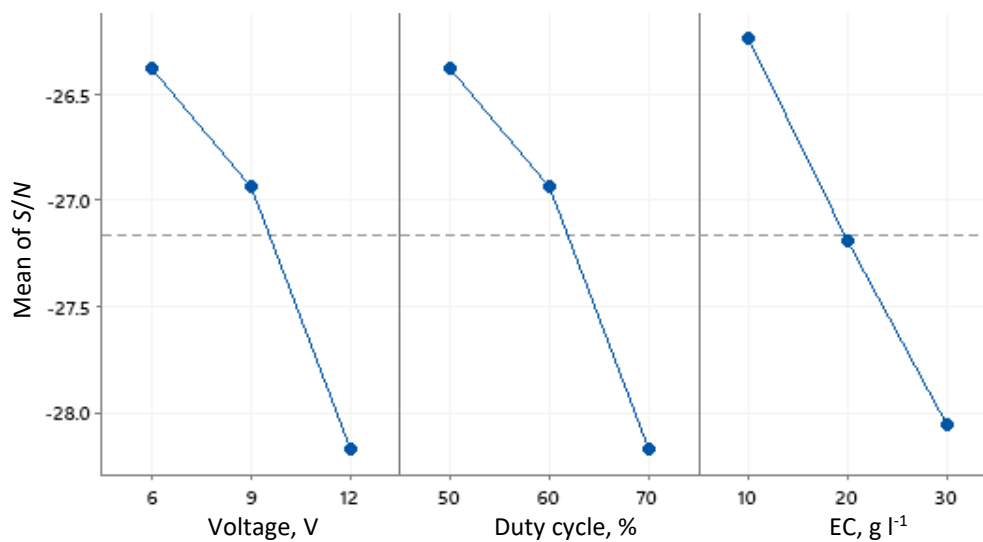
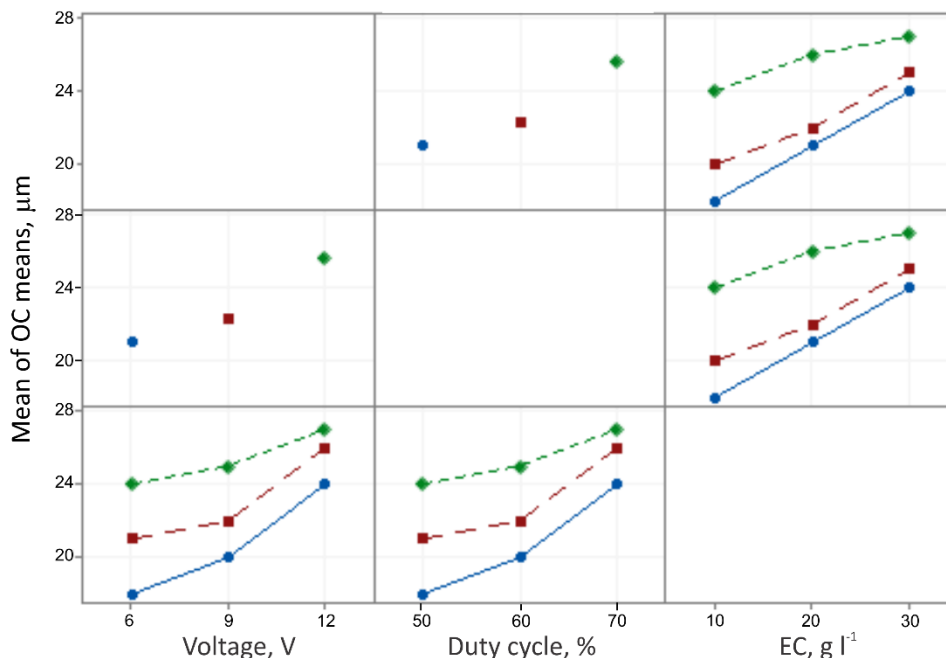


Figure 7. Main effects plots OC-S/N ratio

The interaction plot (Figure 8) demonstrates a moderate interaction between voltage and electrolyte concentration. Although not extremely pronounced, the divergence of lines indicates that the combined effect of high voltage and high electrolyte concentration tends to amplify OC. This is due to synergistic effects where both parameters together intensify the ion flow and material removal beyond the desired area. ANOVA results (Table 4) confirm the statistical significance of both input parameters. Voltage shows a  $p$ -value of 0.005 and electrolyte concentration a  $p$ -value of 0.006, both well below the 0.05 significance thresholds. This clearly indicates that both factors have a significant influence on OC during the ECMM process.



**Figure 8.** Interaction plot of OC

**Table 4.** Analysis of variance-OC

Source	Degree of freedom	Adj SS	Adj MS	F-value	$p$ -value
Voltage	2	34.667	17.3333	26.00	0.005
EC	2	32.667	16.3333	24.50	0.006
Error	4	2.667	0.6667		
Total	8	70.000			

The model summary further validates the reliability of the analysis. The  $R^2$  of 96.19 % indicates that the model explains a very high percentage of the variability in OC. The adjusted  $R^2$  of 92.38 % and predicted  $R^2$  of 80.71 % also support the model accuracy and predictive capability. The optimization results confirm that a voltage of 6 V, a duty cycle of 50 %, and an electrolyte concentration of 10 g l<sup>-1</sup> constitute the most optimal set of process parameters for producing a microhole with minimal OC. Confirmation experiments were conducted using these parameters, and the corresponding SEM image is shown in Figure 9. The use of a lower voltage minimized the effect of stray currents, resulting in a well-defined and precisely machined microhole [22].

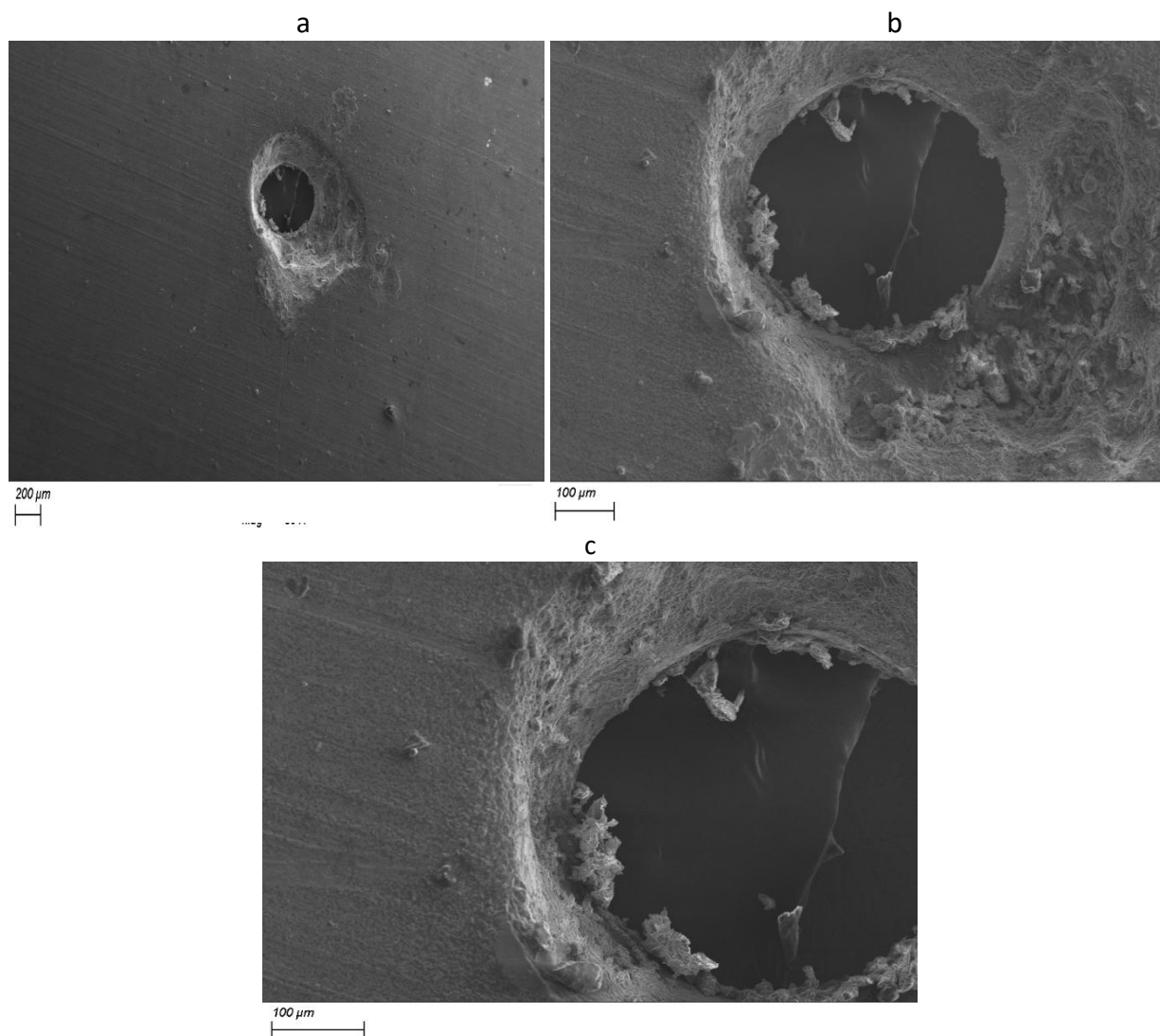


**Figure 9.** SEM images at optimal input parameter-OC: a - machined microhole; b - microhole profile; c - microhole with minimum stray current effect

## Conclusions

This study systematically investigated and optimized the process parameters for electrochemical micromachining of galvanized iron sheets using sodium nitrate ( $\text{NaNO}_3$ ) as the electrolyte. Based on experimental results and statistical analysis, the following key conclusions were drawn: voltage was found to be the most influential parameter affecting both material removal rate and overcut. The maximum MRR of  $1.190 \mu\text{m s}^{-1}$  was achieved at 12 V, 70 % duty cycle and  $10 \text{ g l}^{-1}$  electrolyte concentration. The minimum OC of  $18 \mu\text{m}$  was obtained at 6 V, 50 % duty cycle, and  $10 \text{ g l}^{-1}$   $\text{NaNO}_3$  concentration. Duty cycle played a significant role in controlling machining efficiency. An increase from 50 to 70 % resulted in a noticeable improvement in MRR (up to 59.5 %) but also contributed to increased OC.  $\text{NaNO}_3$  electrolyte concentration had a moderate effect on machining performance. MRR peaked at  $20 \text{ g l}^{-1}$ , while higher concentrations ( $30 \text{ g l}^{-1}$ ) led to slight performance degradation due to increased side reactions and over-etching. SEM analysis confirmed the dimensional and surface quality outcomes, revealing well-defined microholes at lower voltage conditions. The optimized parameters for maximum MRR were 12 V, 70 % duty cycle, and  $20 \text{ g l}^{-1}$   $\text{NaNO}_3$ . For minimal OC, the ideal parameters were 6 V, a 50 % duty cycle, and  $10 \text{ g l}^{-1}$   $\text{NaNO}_3$ . These findings demonstrate that careful tuning of ECMM parameters can achieve a balance between high machining rate and precision, enabling its effective application in the micromachining of galvanized iron components.

## References

- [1] K. P. Rajurkar, M. M. Sundaram, A. P. Malshe, Review of Electrochemical and Electro discharge Machining, *Procedia CIRP* **6** (2013) 13-26. <https://doi.org/10.1016/j.procir.2013.03.002>
- [2] H.-S. Liu, B.-H. Yan, F.-Y. Huang, K.-H. Qiu, A study on the characterization of high nickel alloy micro-holes using micro-EDM and their applications, *Journal of Materials Processing Technology* **169** (2005) 418-426. <https://doi.org/10.1016/j.jmatprotec.2005.04.084>
- [3] A. Kumar, H. N. S. Yadav, M. Kumar, M. Das, Effect of tool rotation on the fabrication of micro-tool by electrochemical micromachining, *Journal of Micromanufacturing* **5** (2021) 217-223. <https://doi.org/10.1177/25165984211031687>
- [4] M. Asmael, A. Memarzadeh, A Review on Recent Achievements and Challenges in Electrochemical Machining of Tungsten Carbide, *Archives of Advanced Engineering Science* **2** (2023) 1-23. <https://doi.org/10.47852/bonviewAAES3202915>
- [5] F. J. G. Silva, Metal Machining-Recent Advances, Applications, and Challenges, *Metals* **11** (2021) 580. <https://doi.org/10.3390/met11040580>
- [6] M. Tomáš, S. Németh, E. Evin, F. Hollý, V. Kundracik, J. M. Kulya, M. Buber, Comparison of Friction Properties of GI Steel Plates with Various Surface Treatments, *Lubricants* **12** (2024) 198. <https://doi.org/10.3390/lubricants12060198>
- [7] P. Rodriguez, D. Hidalgo, J. E. Labarga, Optimization of Pulsed Electrochemical Micromachining in Stainless Steel, *Procedia CIRP* **68** (2018) 426-431. <https://doi.org/10.1016/j.procir.2017.12.090>
- [8] S. Maniraj, R. Thanigaivelan, Effect of electrode heating on performance of electrochemical micromachining, *Materials and Manufacturing Processes* **34** (2019) 1494-1501. <https://doi.org/10.1080/10426914.2019.1655153>
- [9] J. R. Vinod Kumar, R. Thanigaivelan, Performance of magnetic field-assisted citric acid electrolyte on electrochemical micro-machining of SS 316L, *Materials and Manufacturing Processes* **35** (2020) 969-977. <https://doi.org/10.1080/10426914.2020.1750630>
- [10] M. Soundarrajan, R. Thaigaivelan, Effect of coated and geometrically modified tools on performance of electrochemical micromachining, *Materials and Manufacturing Processes* **35** (2020) 775-782. <https://doi.org/10.1080/10426914.2020.1740252>
- [11] P. Venugopal, R. Thanigaivelan, Performance of Magnetized Tool in Electrochemical Micromachining on Scrapped Alloy Wheel Matrix Composite, *Journal of Electrochemical Science and Engineering* **13** (2023) 553-561. <https://doi.org/10.5599/jese.1660>
- [12] Z. Ge, M. Chen, W. Chen, Y. Zhu, Study on Improving Electrochemical Machining Performances through Energy Conversion of Electrolyte Fluid, *Coatings* **14** (2024) 406. <https://doi.org/10.3390/coatings14040406>
- [13] J. Deepak, P. Hariharan, Investigation of electrochemical machining on SS304 using NaCl and NaNO<sub>3</sub> as electrolyte, *Materials and Manufacturing Processes* **37** (2022) 1790-1803. <https://doi.org/10.1080/10426914.2022.2065002>
- [14] N. Sivashankar, R. Thanigaivelan, Performance of Electrochemical Micromachining of Magnesium Alloy Through Sodium Nitrate Electrolyte, in: *Advances in Modern Machining Process, Lecture notes in Mechanical Engineering*, M.S. Shunmugam, B. Doloi, R. Ramesh A.S. Prasanth (Eds.), Springer, Singapore, 2023, 119-128. [https://doi.org/10.1007/978-981-19-7150-1\\_11](https://doi.org/10.1007/978-981-19-7150-1_11)
- [15] N. Sivashankar, R. Thanigaivelan, Electrochemical micromachining of magnesium AZ31 alloy using minimum quantity electrolyte, *Materials and Manufacturing Processes* **38** (2022) 1406-1415. <https://doi.org/10.1080/10426914.2022.2157429>
- [16] S. Ramesh, R. Viswanathan, S. Ambika, Measurement and optimization of surface roughness and tool wear via grey relational analysis, TOPSIS and RSA techniques, *Measurement* **78** (2016) 63-72. <https://doi.org/10.1016/j.measurement.2015.09.036>
- [17] A. Kannan, R. Mohan, R. Viswanathan, N. Sivashankar, Experimental investigation on surface roughness, tool wear and cutting force in turning of hybrid (Al7075 + SiC + Gr) metal matrix composites, *Journal of Materials Research and Technology* **9** (2020) 16529-16540. <https://doi.org/10.1016/j.jmrt.2020.11.074>

- [18] A. Wali, T. Platt, D. Biermann, Fabrication of microcutting tools by pulsed electrochemical machining (PECM), *Production Engineering Research and Development* **19** (2025) 751-761. <https://doi.org/10.1007/s11740-025-01337-y>
- [19] S. S. Deshmukh, K. B. Vinoth, M. Tak, R. G.Mote, Electrochemical micromachining of uniformly tapered needles for endodontic application, *Materials and Manufacturing Processes* **40** (2025) 603-620. <https://doi.org/10.1080/10426914.2025.2462829>
- [20] N. Sivashankar, R. Thanigaivelan, L. Selvarajan, K. Venkataramanan, Investigation of electrochemical micromachining on magnesium alloy using hollow tool electrode, *Ultrasonics* **147** (2025) 107526. <https://doi.org/10.1016/j.ultras.2024.107526>
- [21] T. Geethapriyan, T. Santosh Kumar, R. Sumit Singh, Prem Kumar, K. Gowtham, Experimental investigation of machining rate, geometrical accuracy and optimization of machining parameters in electrochemical micromachining of stainless steel 304, *Journal of Applied Electrochemistry* **55** (2025) 1455-1473. <https://doi.org/10.1007/s10800-024-02254-1>
- [22] N. Pradeep, K. Shanmuga Sundaram, M. Pradeep Kumar, Multi-response optimization of electrochemical micromachining parameters for SS304 using polymer graphite electrode with NaNO<sub>3</sub> electrolyte based on TOPSIS technique, *Journal of the Brazilian Society of Mechanical Sciences and Engineering* **41** (2019) 323. <https://doi.org/10.1007/s40430-019-1823-7>